Advances in Bioresearch
Adv. Biores., Vol 12 (6) November 2021: 169-179
©2021 Society of Education, India
Print ISSN 0976-4585; Online ISSN 2277-1573
Journal's URL:http://www.soeagra.com/abr.html
CODEN: ABRDC3
DOI: 10.15515/abr.0976-4585.12.6.169179

Advances in Bioresearch

ORIGINAL ARTICLE

Investigation of the Interaction of Eugenol with Quercetin Nanoparticles

S.Bakkialakshmi* and S.Pushpa
Department of Physics, Annamalai University, Annamalai Nagar,
Tamilnadu, India-608 002
*Corresponding author E-mail : bakkialakshmis@rocketmail.com

ABSTRACT
The interaction between Eugenol (EG) with Quercetin nanoparticles was investigated by some fluorescence techniques such as, UV/Vis absorption technique, steady – state fluorescence, time – resolved fluorescence, FRET and antibacterial activity. Quercetin nanoparticles were prepared by ionic gelation technique and characterized by UV/Visible, FTIR, XRD, particle size measurement, scanning electron microscope analysis and antibacterial activity. The analysis of the quenching in different concentrations revealed that the quenching mechanism correspond to a static process and as a consequence, a complex formation of eugenol with quercetin nanoparticles were identified. The fluorescence quenching mechanism was conformed by the measurement of synchronous fluorescence and fluorescence lifetime. The distance, r, between donor (eugenol) and acceptor (quercetin nanoparticles) was calculated based on (FRET) theory. The antibacterial activity of the EG/Q Np nanoparticles complex was investigated using Agar well diffusion method.
Keywords: *Eugenol, Quercetin nanoparticles, Fluorescence spectroscopy, Antibacterial Activity.*

Received 16.08.2021 Revised 21.09.2021 Accepted 16.11.2021

How to cite this article:
S.Bakkialakshmi and S.Pushpa. Investigation of the Interaction of Eugenol with Quercetin Nanoparticles. Adv. Biores. Vol 12[6] November 2021: 169-179

INTRODUCTION

Polyphenols are secondary metabolites of plants and, because of their possible health benefits, have gained significant attention [1,2]. It has described and grouped more than 4000 flavonoids according to their molecular structures[3].Nearly every group of flavonoids has the best-described property of their ability to act as antioxidants capable of scavenging free radicals and reactive oxygen species, which are associated with many types of tissue damage and disease, including cancer, atherosclerosis, and aging [3-5].

Quercetin, 3,3',4',5,7-pentahydroxyflavone is generally present in fruits and vegetables, although it occurs at the highest levels in apples and onions in particular [6,7]. Quercetin also exhibits other very important properties, namely: anti-inflammatory[8], anti-atherogenic, and anti-carcinogenic [10], primarily because of its anti-oxidant capacity[11], quercetin is also neuroactive as caffeine and has GRAS (Generally Recognized As Safe) status. Several methods have been reported for quantification of quercetin, namely: spectrophotometry in ethanolic media [6,11] using a coloured complex formed by the reaction of quercetin to aluminum chloride in aqueous media[12] high-performance liquid chromatography [6,11] electrochemistry [7,13,14] photo-electrochemical [15].

Quercetin, which includes a -OH group at position 5 (C-5), flavonols form a special class of aqueous solution non-fluorescent molecules; since the intermolecular hydrogen bond between the polar solvent groups and H_2O exceeds different intramolecular hydrogen bonds, it reveals a wide dihedral angle that makes it very difficult for ESICT (excited state intramolecular charge transfer) to occur. Eugenol (EG, 2-methoxy-4-(2-propenylphenol) is a plant-derived natural flavor extract and is commonly used in a variety of cosmetics and food products as a fragrant and flavoring agent. [16,17] Different biological activities are well known, such as antibacterial, antifungal [18] and antioxidant [17] properties in particular. A great deal of attention has been given to the role of such molecules in disease prevention and therapy[19]. Besides, the Food and Drug Administration has demonstrated its antifungal and antibacterial

habitat properties and applications [20, 21]. Their poor water solubility, however, restricts their applications and bioavailability. Besides, when exposed to air, light, or heat, EG oil is easily oxidized, decomposed, or evaporated. One way these compounds can be stabilized and used is by integrating them into acceptable host molecules.

MATERIAL AND METHODS

Eugenol and quercetin were purchased from Sigma–Aldrich, Bangalore. Low molecular weight Chitosan(CS) and sodium tripolyphosphate were purchased from Sisco research laboratory, Chennai.

Preparation of Quercetin Nanosuspension and Optimization of Preparation Process

Nanosuspension with relevant stabilizer was prepared by ionic gelation method. Chitosan solution (0.1%w/v) was prepared by dissolving chitosan in 100 ml of 1%v/v of acetic acid, and the resulting solution was stirred at 1500 rpm for 30 min on magnetic stirrer. TPP solution of 0.1% was prepared by dissolving 100 mg of TPP in 100 ml of deionized water. 100 mg of quercetin was added to TPP solution and mix to form a homogenous mixture by stirring with a glass rod. Add the above mixture of TPP and hesperidin solution drop by drop (10 ml) to the chitosan solution and kept stirring at 2,500 rpm for 3 h on mechanical stirrer. By adding a solution of TPP and quercetin to a solution of chitosan, nanoparticles were obtained. Discard the sediment and the supernatant is retained. The formation of nanoparticles results in an interaction between the negative TPP groups and the chitosan amino groups that are positively charged.

Characterization of Quercetin -Loaded Chitosan Nanoparticles

Particle Size

The size of the prepared nanoparticles was analyzed using (MICROMRTICS CPE-11 Nano plus).

Fourier-transform infrared (FTIR) study

FTIR analysis of pure quercetin mixture (quercetin, chitosan, and TPP) was performed, and the spectrum was obtained using FT-IR (IR spectrometer Agilent Cary-630 FTIR Technology). All spectra were recorded within a range of 4000–500 cm^{-1}.

SEM analysis

The SEM photographs of Quercetin Nanoparticles were captured with the Joel Sem Model, Jsm-IT 200 Scanning Electron Microscope.

XRD

The XRD for Q-Np analyzed by X-Ray Diffractometer (BRUCKER D8 Advance).

METHODS

Experiments of UV/Vis absorption

Using the SHIMADZU 1800 PC UV/Visible Spectrophotometer, the absorption spectra of Eugenol and in different concentrations of quercetin nanoparticles were reported.

Fluorescence steady – state measurements

A Shimadzu RF 5301PC Spectrofluorophotometer was used to conduct the steady-state fluorescence quenching measurements.280 nm was the excitation wavelength. At 317nm, the emission wavelength was controlled.For all the experiments, the excitation and emission slit widths (5nm) and scan rate (200 nm/s) were constantly maintained.

Fluorescence lifetime measurement

In the Hariba-Jobin Yvon[spex-sf13-11] Spectrofluorimeter, fluorescence lifetime measurements were performed.As an excitation source, an interchangeable nano LED (280 nm) was used.With a monochromator-Photo Multiplier Setup, the fluorescence decay of Eugenol was measured.

Antibacterial Activity

The samples(0.5g) were dissolved in 1ml DMSO. The antimicrobial activity screening was performed with the Muller Hinton agar (MHA) medium for antibacterial activity in the agar well diffusion method. The fungal and bacterial inocula have been prepared on the nutrient broth medium from 24-hour colonies. The inoculum with McFarland density had been adjusted to obtain a final bacterial density of around 10^4 and 10^6 CFU/mL. In Whatmann AA filter paper, 50µg each extract was imbibed and applied to the test media previously inoculated with each test strain. Plates for bacteria have been incubated at 37°C. Zones of inhibition were measured after 24 hours of incubation [22].

RESULTS AND DISCUSSION

Characterization of Quercetin nanoparticles

The formed chitosan nanoparticles were characterized using UV, FTIR, Scanning electron microscope (SEM), XRD and Particle size analyser.

UV – Visible Spectroscopy

UV - Visible spectrometry is the main technique to examine size and shape of the nanoparticles. As these nanoparticles exhibit an extreme peak of absorption due to the excitation of the surface plasmon, it is very sensitive to the presence of colloids. The SHIMADZU 1800 PC UV/Visible Spectrophotometer was used to conduct the UV-Visible Spectral analysis. A tiny aliquot was drawn from the reaction mixture and a wavelength range from 200 nm to 800 nm was taken. The UV-Visible results show a typical absorption peak of quercetin at 264 as results are expressed in Figure 1

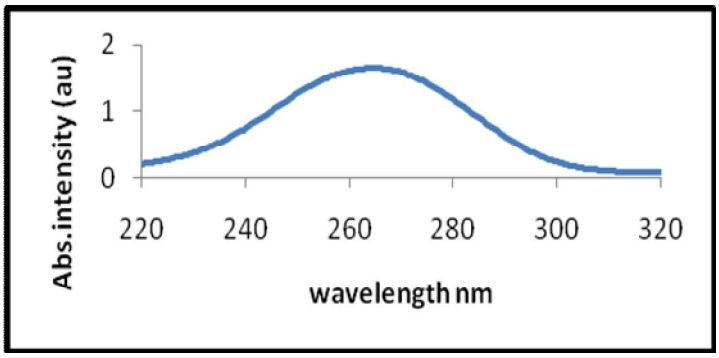

Figure 1: UV/Vis absorption spectra of Quercetin nanoparticles

Fourier transform infrared spectroscopy

The chemical composition of many organic chemicals, polymers, coatings, paints, adhesives, semiconductor materials, lubricants, gages, coolants, biological samples, inorganics and minerals can be examined using FTIR. A wide variety of materials in bulk or their liquids, films, pastes, solids, fibers, powders and other types can be examined using FTIR [23]. Information about the local molecular environment of organic molecules on the surface of nanoparticles was given by the FTIR spectrum. FTIR analysis can provide not only qualitative (identification) analysis of materials but with appropriate criteria, can be used for quantitative (amount) analysis.

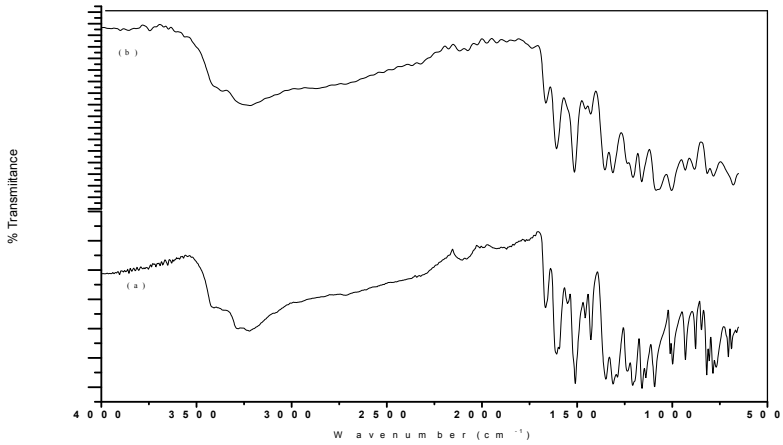

Figure2: FTIR spectra of (a) quercetin (b) quercetin nanoparticles

The quercetin nanoparticles exhibit intense absorption peaks (Table 1) at 3407 corresponded to O-H Stretching of alcohol group. The band absorbed at 2971 exhibits C-H Streching of alkane group. The absorption band at 2323 corresponded to O-H hydroxyl bond. The other absorption peak at 1139 corresponded to C-O Stretching of ether group as results are expressed in Figure 2.

Table 1: FTIR peak assignments of Quercetin, Quercetin nanoparticles complex

Q (cm^{-1})	Q nanoparticle (cm^{-1})	Peak Assignments
3407.25	3363.26	OH stretching
2971.65	2871.66	C-H stretching
2322.18	2323.24	O-H hydroxyl bond
1139.04	1003.35	C- O stretching

Scanning Electron Microscopy

SEM was applied to evaluate the surface morphologies of the nanoparticles. SEM images at different magnifications were obtained. A fine, highly concentrated beam of electrons is screened over a thin specimen and the electrons that pass through the thin sample are captured on a detector mounted underneath the sample, yielding the desired bright - field images.

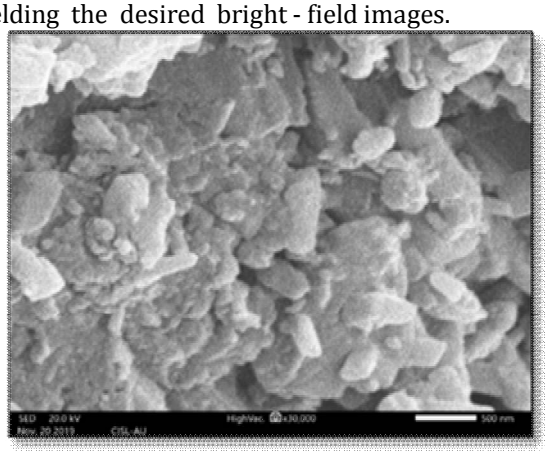

Figure3: SEM image of Quercetin nanoparticles

The SEM image (Figure 3) showed somewhat spherical shaped nanoparticle. The electrons transmitted are guided by an electron multiplier, i.e., a gold layer, onto a conventional detector.

XRD Analysis

An x ray diffractometer was used to estimate the crystalline state of the samples. The XRD Patterns of the quercetin at flow rate (8 and 10 ml /min) and the sample displayed the presence of the numerous distinct peaks at 2θ (38.75) which suggested that the quercetin was of a high crystalline form as results are expressed in (Figure 4)

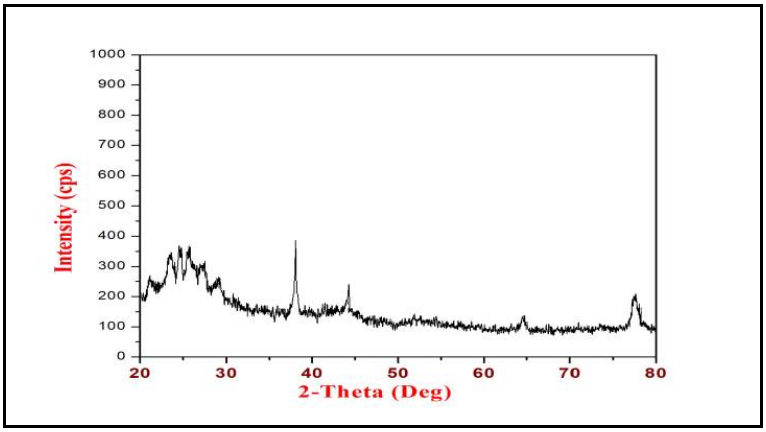

Figure 4: XRD spectra of Quercetin nanoparticles

Particle size analyser

The particle size was obtained using particle size analyzer. At 25˚C temperature, the observation was performed with water as the solvent.As a consequence of this finding, the average particle size of the formulation of quercetin is 330.3 nm (Figure 5) obtained particles have size range in nanometer, as aimed. Colloid nanoparticle has several beneficial properties, namely that nano-size steadily makes it much more stable to sediment.

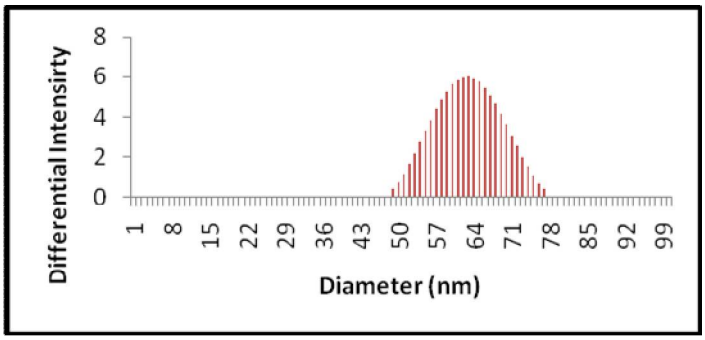

Figure 5: Particle size analyser of Quercetin nanoparticles

The index of polydispersibility obtained from the particle size calculation was 0.374. The polydispersibility index defines the distribution of the particle sizes present in the preparation of nanoparticles, the smaller the polydispersibility index, the more uniform the particle sizes, and if there is a substantial difference in size between the larger and smaller particles, the characteristic of the particles will be affected. The larger the particle size, the better it can settle for the particle. The interaction study of Eugenol with the quercetin nanoparticles (above said prepared and characterized) has been carried out by using the UV - Visible, Fluorescence, Synchronous fluorescence, FRET, Lifetime and antibacterial activity . This interaction study has been discussed below.

Absorption and Fluorescence Spectra

Figure 6 Presents the absorption spectra of Eugenol without and with different concentrations of quercetin nanoparticles. Free Eugenol shows absorption peaks at 280 nm. The addition of quercetin nanoparticles leads to increased eugenol absorption with the same peaks. This indicate the potential Eugenol – quercetin nanoparticle complex formation.

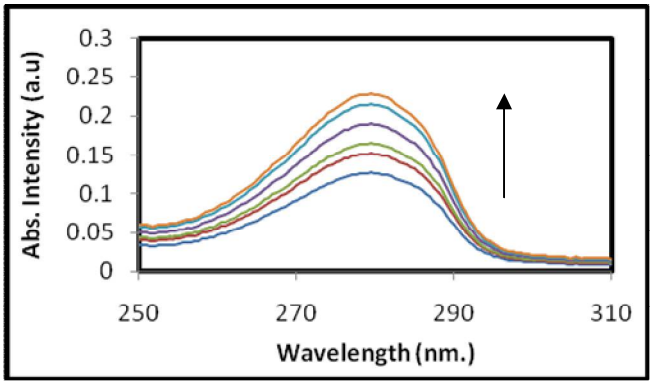

Figure 6: UV/Vis absorption spectra of Eugenol with different concentrations of Quercetin nanoparticles (mol L^{-1}) (1)0, (2)0.2, (3)0.4, (4) 0.6, (5) 0.8, (6) 1.0.

Steady-state measurements of the solutions containing fixed quantities of Eugenol and varying concentrations of quercetin nanoparticles have further examined the investigation. (0 to1.0 ML^{-1}). The sample with the lowest concentration of quercetin (0.2 ML^{-1}) has a maximum of 280 nm in the absorption spectrum. Increasing the content of nanoparticles with quercetin results in greater absorption. In the study of molecular interaction between ligands and proteins, fluorescence spectroscopy has generally been used, mainly due to the high sensitivity of this methodological approach and the variety of parameters related to the molecular interaction that can be obtained. Quenching fluorescence measurements were performed to obtain precise information about the interaction of Eugenol-Quercetin nanoparticles. Figure 7 shows Eugenol emission spectra in the absence and presence of concentrations of quercetin ranging from 0 to 1.0 ML^{-1}. Increasing concentrations of quercetin will lead to a regular quenching of Eugenol fluorescence without changing the maximum emission from Figure 7.

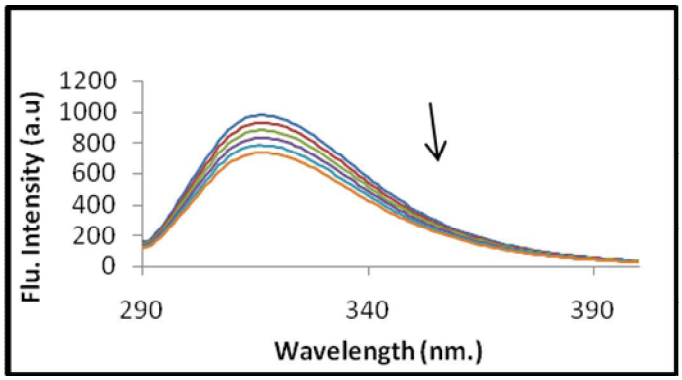

Figure 7: Steady–State fluorescence spectra of EG with different concentrations of Quercetin nanoparticles (mol L^{-1}) (1) 0, (2) 0.2, (3) 0.4, (4) 0.6, (5) 0.8, (6) 1.0 .

Fluorescence quenching can occur through two separate mechanisms that are known as static or dynamic quenching. It is possible to differentiate these processes by their varying temperature dependence. The quenching rate constant decreased with the increased temperature for the state mechanism and the opposite effect is observed for the dynamic quenching event. In order to determine the form of mechanism, Eugenol fluorescence data were plotted against quercetin concentration as relative fluorescence intensity (F_0/F), F and F_0 being the fluorescence intensity in the presence and absence of nanoparticles of quercetin respectively. From the Stern-Volmer plot, the quenching constants were obtained by linear regression using the expression.

$$F_0 / F = 1 + K_q \tau_0 [Q] = 1 + K_{SV} [Q] \quad (1)$$

Where k_q is the constant of bimolecular quenching, K_{SV} is the constant of stern-volume quenching and the lifetime of the fluorophore in the absence of a quencher equal to 10^{-8} s [24]. It is possible to deduce the possible mechanism from the Stern-Volmer plots [25], as shown in Figure 8. The experimental data obtained were tabulated in Table.2.

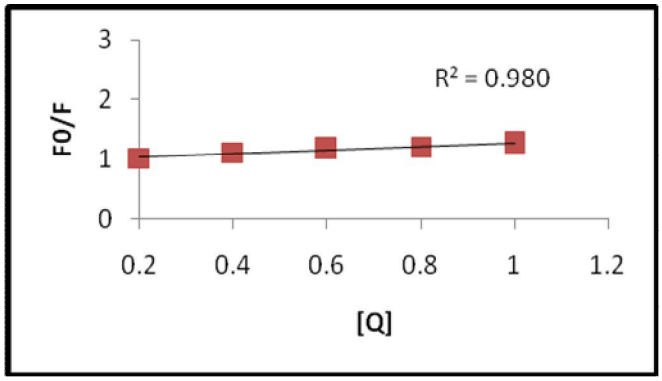

Figure 8: Stern-Volmer plot of EG with Quercetin nanoparticles

Table 2: Stern – Volmer (K_{SV}) and bimolecular quenching rate constant (K_q) of Eugenol with quercetin nanoparticles

Quencher	K_{SV} x 10^5 (L mol^{-1})	K_q (L mol^1S^{-1})	R[a]	S.D[b]
Quercetin nanoparticles	0.21	1.15	0.9	0.36

It is recognized that the maximum scatter collision quenching constant for a dynamic mechanism is 2.0×10^{10} L mol^{-1} s^{-1} [26]. The rate constants obtained for quercetin-induced Eugenol quenching are greater than the rate limit for dynamic quenching and, as a result, the quercetin-induced quenching mechanism is of a static form with great probability. The results obtained indicate the development of a complex of nonfluorescent Eugenol-quercetin nanoparticles. If it has been assumed that there are n possible binding sites for quercetin nanoparticles (QNP) on Eugenol, the reaction for complex formation may be,

$$n\ QNP + E \longleftrightarrow QNP_nE \quad (2)$$

Being the binding constant k_B.

$$K_B = \frac{[QNP_n E]}{[QNP]^n [E]} \quad (3)$$

Where, [QNP], [E] and [QNP_n E] are the quercetin nanoparticles, Eugenol and complex concentrations respectively. If total Eugenol concentration is [E_0], then [QNP_n E] = [E_0] - [E] and by substiluation in (3) ,

$$K_B = \frac{[E_0] - [E]}{[QNP]^n [E]} \quad (4)$$

If the fluorescence intensity of eugenol has been found to be proportional to its concentration,

$$\frac{[E]}{[E_0]} = \frac{F}{F_0} \quad (5)$$

and by substitution in (4) the following expression (6) has been obtained [17]

$$\log (F_0 - F) / F = \log K_B + n \log [Q] \quad (6)$$

The values for K_B and n can be obtained from (6) , plotting log [(F_0 – F)/ F] VS log [Q] and determining the intercept and slope as shown in Figure 9. The results obtained from this plot are presented in Table 3.

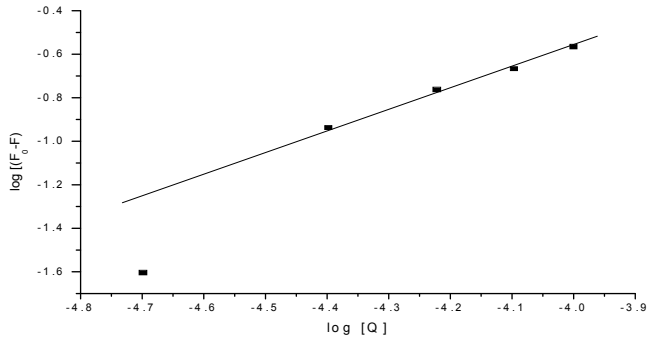

Figure 9: Double log plot of EG with Quercetin nanoparticles

Table 3: Formation constant K_e (M^{-1}) and free energy ΔG_e (kJ mol^{-1}) of eugenol with quercetin nanoparticles

Quencher	K_e (M^{-1}) x 10^{-3}	ΔG_e (kJ mol^{-1}) x 10^4	R[a]	S.D[b]
Quercetin nanoparticles	2.4	1.51	0.9	0.3

Nanoparticles with quercetin are binding in a ratio of 1:1 in n, almost 1 as shown by the value obtained for n. The creation of a relatively stable complex can be deduced from the K_B value.

Binding Distance between quercetin nanoparticles and Eugenol

For determining the distance between the fluorescent donor (Eugenol) and an accepter, the non-readable Forster energy transfer may be used (quercetin nanoparticles). when the donor fluorescence emission spectrum overlaps the accepter UV absorption spectrum is possible this transfer possible.

Figure 10. shows the overlap of the uv absorption spectrum of quercetin nanoparticles with the fluorescence emission spectrum of eugenol. The efficiency of energy transference was calculated according Forster energy transference theory [27] using the eqn (7)

$$E = \frac{R_0^6}{(R_0^6 + r^6)} = 1 - \left(\frac{F}{F_0}\right) \quad (7)$$

If F and F_0 are the strength of fluorescence of eugenol in presence and absence of quercetin nanoparticles, r is the distance between the donor and the accepter and R_0 is the distance of 50 percent from the eqn (8)

$$R_0^6 = 8.79 \times 10^{-25} K^2 n^{-4} \phi J \quad (8)$$

Where K^2 is the dipole's spectral orientation factor, n is the medium's refractive index, φ is the donor's fluorescence quantum yield, and J is the spectral overlap between donor emission and acceptor absorption eqn (9)

$$J = \frac{\int_0^{\alpha} F(\lambda(\Sigma(\lambda)\lambda^4 \Delta\lambda}{\int_0^{\alpha} F(\lambda(\Delta\lambda} \qquad (9)$$

being F(λ) the fluorescence intensity of donor at the wavelength λ, Σ(λ) is the molar absorption coefficient of the acceptor at the wavelength λ. Data for the determination of J were obtained from the spectra of Figure10.

From experimental data, the values determined are R_0= 2.2 nm and r=1.9 nm. The donor – acceptor, r, has a value in the range 2-8 nm, indicating that the energy transfer from eugenol to quercetin nanoparticles is highly likely and that there is an interaction with the formation of a complex donor – acceptor responsible for static quenching.

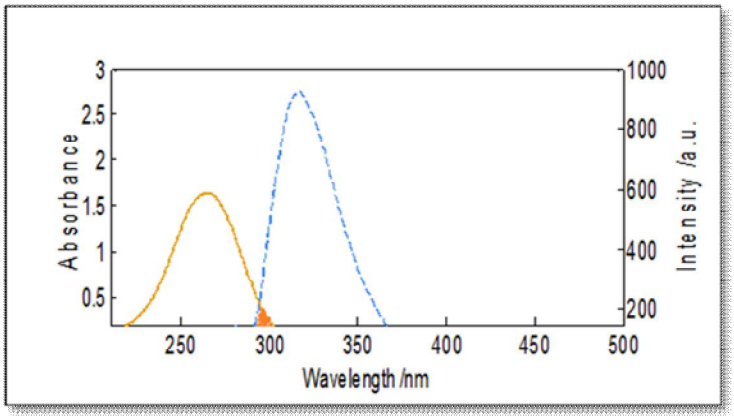

Figure10: The overlap of UV absorption spectra of Quercetin– NP (solid line) with the fluorescence emission spectra of Eugenol (dotted line)

Conformational Investigation

In order to explore the structural change of eugenol by the addition of quercetin nanoparticles, Eugenol synchronous fluorescence spectra with different concentrations of quercetin nanoparticles have been measured. (Figure.11).Synchronous fluorescence is a kind of simple and effective means of measuring the quenching of fluorescence and the possible shifting of the maximum emission wavelength λ_{max}, relative to the alteration of the polarity around the microenvironment of chromophore, Δλ, representing the difference between excitation and emission wavelength is an important operating parameter.

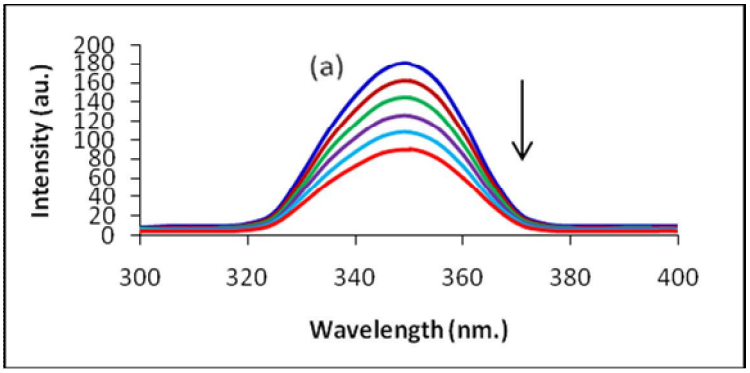

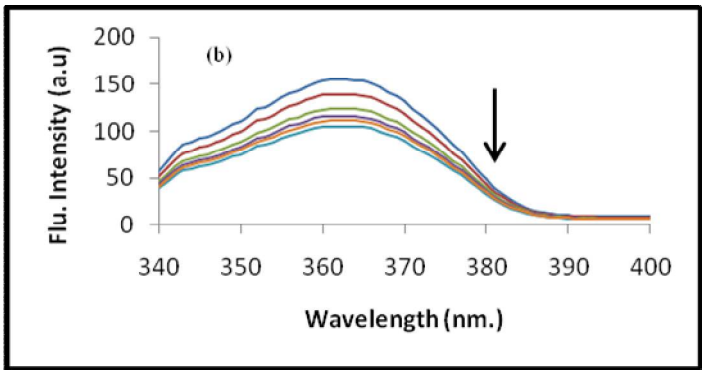

Figure11**:** Synchronous Fluorescence Spectra for EG with quercetin nanoparticles
(a) Δλ = 30 (b) Δλ = 60 nm

When the Δλ is 30 and 60 nm, the spectral character of Eugenol displays the synchronous fluorescence spectrometry. The λ_{max} change and Eugenol fluorescence tearing require an attraction to the microenvironnement of the polarity and binding state when Δλ is at a temperature of 30 nm or at 60 nm. But if the Δλ is 60 nm, then the decline in fluorescence is much greater than 30 nm.

Fluorescence lifetime measurements

The measurements of fluorescence lifetime were also carried out. The lifetimes of fluorescence have been measured with a time-related single photon count spectrometer. Decay curves were fitted using a nonlinear iterative least square fit method using the following,

$$G(t) = \Sigma_i B_i \exp(-t/t_i) \quad (10)$$

G (t) is the curve of decay in order that Bi is the pre-exponential factor in the i^{th} component, and that δ_i is the corresponding fluorescence lifetime.

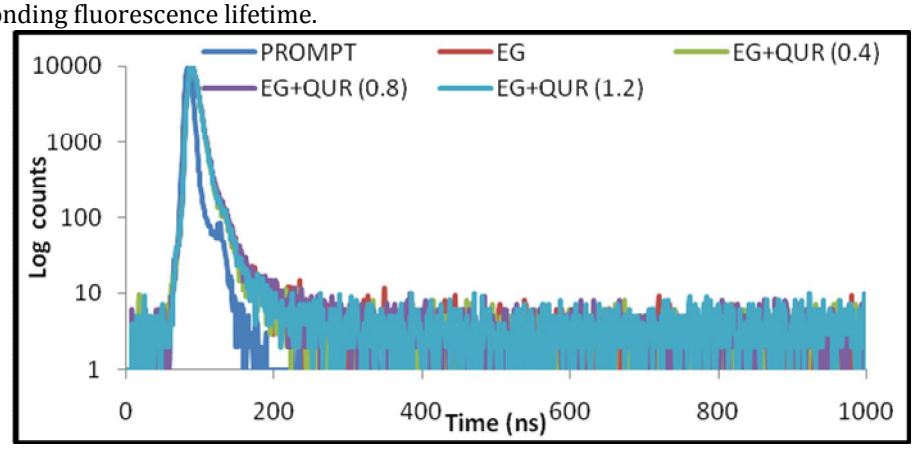

. Figure 12**:** Time-resolved fluorescence spectra of Eugenol (EG) with different concentrations of Quercetin Nanoparticles (mol dm^{-4}) (1)0, (2) 0.4, (3) 0.8, (4) 1.2

On the basis of the reduced λ^2 values (1.00-1.15) and the distribution of weighted waste (random) through the data channels, bi exponential or tri-exponential nature of decays has been measured (28).

In the absence and presence of quercetin nanoparticles, time –resolved measurements of Fluorescence lifetime for eugenol have been carried out. (Figure12) Multiple exponential functions could be fitted with fluorescence decay for Eugenol.

Table 4: Time-resolved fluorescence spectra of Eugenol (EG) with different concentrations of Quercetin Nanoparticles (mol dm^{-4}) (1)0, (2) 0.4, (3) 0.8, (4) 1.2

Concentration (M)	Lifetime (ns)		Average life time x 10^{-9} sec	Relative amplitude		χ^2	S.D 10^{-11} sec	
	τ_1	τ_2		B_1	B_2		τ_1	τ_2
EG	6.65	4.35	0.75	97.69	2.31	1.17	4.45	2.11
EG + Q(0.4)	6.67	5.23	0.74	98.2	1.72	1.08	4.17	3.26
EG + Q(0.8)	4.89	6.51	0.69	0.99	99.01	1.05	5.35	4.03
EG + Q(1.2)	6.32	3.59	0.68	98.33	1.67	1.21	5.80	2.89

Antibacterial Activity

The terpene components of essential oils interrupt the bacterial membrane of bacteria and thus essential

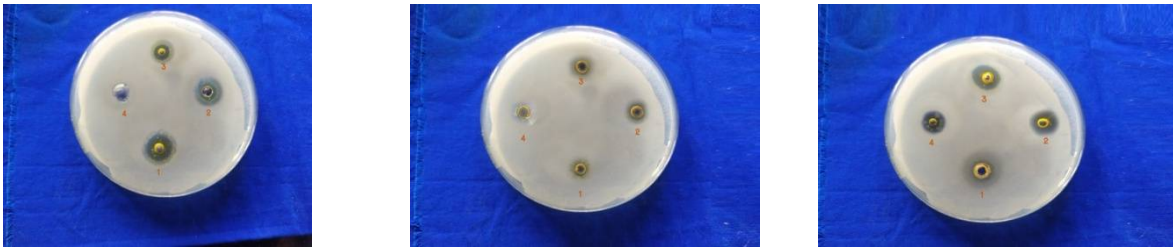

(a) (b) (c)

Figure 13: The antibacterial activity of (a) Eugenol (b) Quercetin (c) Eugenol-Quercetin nanoparticles (1.staphyloccus sp., 2.E.Coli, 3.V.B, 4.Salmonella sp.)

oils exhibit antibacterial activity (29). The antibacterial activity of quercetin nanoparticles–Eugenol was checked by using the agar well diffusion process. (Figure 13). The sample had good antibacterial activity, as can be seen in the plates. Eugenol quercetin nanoparticles, in short, are effective Gram-negative and Gram-positive antibacterial materials.

CONCLUSION

The Desolvation and ionic gelation process used to prepare quercetin and chitosan nanoparticles, which has been verified, by UV, FTIR, SEM, XRD and Particle size analyser. The binding interaction of quercetin nanoparticles eugenol was studied by different spectroscopic techniques. The quenching fluorescence analysis shows clearly that a complex format and static mechanism exist between quercetin nanoparticles and eugenol. According to Forster theory of non-radioactive energy transfer, the binding distance, r, quercetin and eugenol have been calculated and the value obtained confirms the creation of a stable complex.

REFERENCES

1. Papadopoulou A, Green RJ, Frazier RA. (2005). Interaction of flavonoids with bovine serum albumin: a fluorescence quenching study. Journal of agricultural and food chemistry. 53(1):158-63.
2. Duthie GG, Duthie SJ, Kyle JA. (2000). Plant polyphenols in cancer and heart disease: implications as nutritional antioxidants. Nutrition research reviews. 13(1):79-106.
3. Wilmsen PK, Spada DS, Salvador M. (2005). Antioxidant activity of the flavonoid hesperidin in chemical and biological systems. Journal of agricultural and food chemistry. 15;53(12):4757-61.
4. Nijveldt RJ, Van Nood EL, Van Hoorn DE, Boelens PG, Van Norren K, Van Leeuwen PA. (2001). Flavonoids: a review of probable mechanisms of action and potential applications. The American journal of clinical nutrition. 74(4):418-25.
5. Jung HA, Jung MJ, Kim JY, Chung HY, Choi JS. (2003). Inhibitory activity of flavonoids from Prunus davidiana and other flavonoids on total ROS and hydroxyl radical generation. Archives of pharmacal research. 26(10):809-15.
6. Lombard KA, Geoffriau E, Peffley E. (2002). Flavonoid quantification in onion by spectrophotometric and high performance liquid chromatography analysis. HortScience. 37(4):682-5.
7. Gutiérrez F, Ortega G, Cabrera JL, Rubianes MD, Rivas GA. (2010). Quantification of quercetin using glassy carbon electrodes modified with multiwalled carbon nanotubes dispersed in polyethylenimine and polyacrylic acid. Electroanalysis. 22(22):2650-7.
8. Álvarez-Diduk R, Ramírez-Silva MT, Galano A, Merkoçi A. (2013). Deprotonation mechanism and acidity constants in aqueous solution of flavonols: a combined experimental and theoretical study. The Journal of Physical Chemistry B. 117(41):12347-59.
9. Rotelli AE, Guardia T, Juárez AO, De la Rocha NE, Pelzer LE. (2003). Comparative study of flavonoids in experimental models of inflammation. Pharmacological research. 48(6):601-6.
10. Verma AK, Johnson JA, Gould MN, Tanner MA. (1988). Inhibition of 7, 12-dimethylbenz (a) anthracene-and N-nitrosomethylurea-induced rat mammary cancer by dietary flavonol quercetin. Cancer research. 48(20):5754-8.
11. Yoo KS, Lee EJ, Patil BS. (2010). Quantification of quercetin glycosides in 6 onion cultivars and comparisons of hydrolysis-HPLC and spectrophotometric methods in measuring total quercetin concentrations. Journal of food science. 75(2):C160-5.
12. Dowd LE. (1959). Spectrophotometric determination of quercetin. Analytical Chemistry. 31(7):1184-7.
13. Álvarez-Diduk R, Ramírez-Silva MT, Alarcon-Angeles G, Galano A, Rojas-Hernandez A, Romero-Romo M, Palomar-Pardave M. (2009). Electrochemical Characterization of Quercetin in Aqueous Solution Analysis. ECS Trans. 20:115–122.

14. Lu B, Xia J, Wang Z, Zhang F, Yang M, Li Y, Xia Y. (2015). Molecularly imprinted electrochemical sensor based on an electrode modified with an imprinted pyrrole film immobilized on a b-cyclodextrin/gold nanoparticles/ graphene layer. RSC Adv. 5: 82930–82935.
15. Tian L, Wang B, Chen R, Gao Y, Chen Y, Li T. (2015). Determination of quercetin using a photo-electrochemical sensor modified with titanium dioxide and a platinum (II)-porphyrin complex. Microchimica Acta. 182(3):687-93.
16. Siano F, Ghizzoni C, Gionfriddo F, Colombo E, Servillo L, Castaldo D. (2003). Determination of estragole, safrole and eugenol methyl ether in food products. Food chemistry. 81(3):469-75.
17. Atsumi T, Fujisawa S, Tonosaki K. (2005). A comparative study of the antioxidant/prooxidant activities of eugenol and isoeugenol with various concentrations and oxidation conditions. Toxicol. In Vitro. 19: 1025–1033
18. Cheng SS, Liu JY, Chang EH, Chang ST. (2008). Antifungal activity of cinnamaldehyde and eugenol congeners against wood-rot fungi. Bioresource technology. 99(11):5145-9.
19. Aggarwal BB, Shishodia S. (2006). Molecular targets of dietary agents for prevention and therapy of cancer. Biochemical pharmacology. 71(10):1397-421.
20. Sheu WH. Ou HC, Chou FP, Lin TM, Yang CH. (2006). Rosiglitazone inhibits endothelial proliferation and angiogenesis. Life Sci. 78:1520-8.
21. Opdyke DL. Monographs on fragrance raw materials. (1975). Food and cosmetics toxicology. 13(4):449-57.
22. Galeano E, Martínez A. (2007). Antimicrobial activity of marine sponges from Urabá Gulf, Colombian Caribbean region. Journal de Mycologie Médicale. 17(1):21-4.
23. Yao H, Kumura K. (2007). Field Emission Scanning Electron Microscopy for Structural Characterization of 3D Gold Nanoparticle superlattices.Formatex: Mordern Research and Educational Topics in Microscopy. 569.
24. Gutzeit HO, Henker Y, Kind B, Franz A. (2004). Specific interactions of quercetin and other flavonoids with target proteins are revealed by elicited fluorescence. Biochemical and biophysical research communications. 318(2):490-5.
25. Sengupta B, Banerjee A, Sengupta PK. (2005). Interactions of the plant flavonoid fisetin with macromolecular targets: insights from fluorescence spectroscopic studies. Journal of Photochemistry and Photobiology B: Biology. 80(2):79-86.
26. Zsila F, Bikádi Z, Simonyi M. (2003). Probing the binding of the flavonoid, quercetin to human serum albumin by circular dichroism, electronic absorption spectroscopy and molecular modelling methods. Biochemical pharmacology. 65(3):447-56.
27. Gutzeit HO, Henker Y, Kind B, Franz A. (2004). Specific interactions of quercetin and other flavonoids with target proteins are revealed by elicited fluorescence. Biochemical and biophysical research communications. 318(2):490-5.
28. Sytnik A, Litvinyuk I. (1996). Energy transfer to a proton-transfer fluorescence probe: tryptophan to a flavonol in human serum albumin. Proceedings of the National Academy of Sciences. 93(23):12959-63.
29. Delaquis PJ, Stanich K, Girard B, Mazza G. (2002). Antimicrobial activity of individual and mixed fractions of dill, cilantro, coriander and eucalyptus essential oils. International journal of food microbiology. 74(1-2):101-9.